Final project: "Stacking for improving neural optimal transport based style-transfer models"

Daniil Panov [1] **Anastasia Gavrish** [1] **Nikita Bogdanov** [1] **Nikita Vasilev** [1] **Nikolay Kashin** [1]

Abstract

In this project, a stacking approach has been applied to a neural optimal transport (NOT) problem of image style transfer. The main objective is to evaluate the effect of stacking on improving the NOT performance. The stacking was done over the strong neural optimal transport realization of (Korotin et al., 2022). The stacking was applied to the shoe to bag style transfer problem. The unpaired data sets were taken from open sources. The evaluation of the results was done based on Frechet Inception Distance (FID). Up to three iterations of stacking were performed to see which of the iterations would have the lowest FID score.

Github repo: our project github repo link here

1. Introduction

The solution of the problem of finding the optimal way of moving a distribution of mass were proposed as large-scale OT (Seguy et al., 2017) and Wasserstein GANs (Arjovsky et al., 2017). In most of the methods for solving OT, the loss is calculated and used in updating the generator in generative models (Gulrajani et al., 2017; Liu et al., 2017; Sanjabi et al., 2018; Petzka et al., 2017). One of the most recent works presents the neural network based algorithms to compute optimal transport maps and plans for strong and weak transport costs (Korotin et al., 2022).

Existing methods are designed only for strong OT formulation. Most of them search for a deterministic solution, i.e. a map $T^\star$, rather than a stochastic plan $\pi^\star$, even though $T^\star$ may not always exist.

To compute the OT plan (map), (Lu et al., 2020; Xie et al., 2019) approach the primal formulation. Their methods imply the use of generative models and yield complex optimization objectives with multiple adversarial regularizers, e.g., they are used to enforce the boundary condition $(T_\# P = Q)$. As a result, these methods are difficult to tune because they require careful selection of hyperparameters.

In contrast, methods based on the dual formulation have simpler optimization procedures. Most of these methods are designed for OT with quadratic cost, i.e., the Wasserstein-2 distance (W_2^2). An evaluation of these methods is given in (Korotin et al., 2021a).

Recently, the optimal transport has been applied to the image-to-image style transfer problem. In image-to-image style transfer, optimal transport can be used to compare the statistical properties of the input and reference images, such as color histograms or texture distributions. By comparing these properties, optimal transport can find an optimal mapping between the input and reference images that minimizes the distance between their distributions. Application of neural optimal transport to the problem was demonstrated by (Korotin et al., 2022).

Besides the high potential of the application of the neural optimal transport, it is still can produce artifacts or defects in the image. In the report, we propose the stacking of some neural optimal transport models to increase the performance of the NOT.

1.1. The main contributions of this report

- In Section "Algorithms and Models", we provide a theoretical description of what loss function is used and how the stacking is applied for model improvement.
- In Section "Experiments and Results.", we show how stacking influence our predictions. Also data and its preprocessing is described.

2. Algorithms and Models

In our project we use the following experimental setup for numerical experiments: a premium Google Colab and a home personal computer. The source code and requirements could be found in the project Github repository (GitHub).

In this section, we introduce some concepts of strong Opti-

[1]Skolkovo Institute of Science and Technology, Moscow, Russia. Correspondence to: Nikita Gushchin <Nikita.Gushchin@skoltech.ru>.

Final Projects of the Machine Learning 2020 Course, Skoltech, Moscow, Russian Federation, 2020.

mal Transport (OT) theory.

Notations. We use X, Y, Z to denote Polish spaces and $P(X), P(Y), P(Z)$ to denote the respective sets of of probability distributions on them. We denote the set of probability distributions on X × Y with marginals P and Q by $\Pi(P, Q)$. For a measurable map $T : X \times Z \to Y$ (or $T : X \to Y$),

Strong OT formulation. For $\mathbb{P} \in P(X)$, $\mathbb{Q} \in P(Y)$ and a cost function $c : X \times Y \to R$, Monge's Primal formulation of OT cost is:

$$Cost(\mathbb{P}, \mathbb{Q}) = \inf_T \int_\chi c(x, T(x))\, d\mathbb{P}(x) \tag{1}$$

where the minimum is taken over measurable functions (transport maps) $T : X \to Y$ that map P to Q (Figure 1).

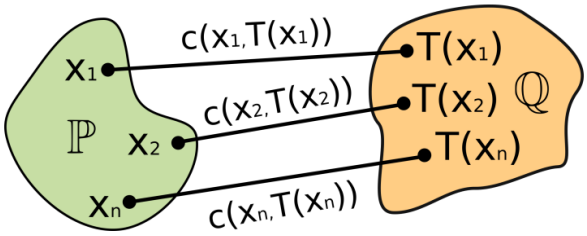

Figure 1. Monge's OT formulation (Korotin et al., 2022)

The optimal T^* is called the OT map.

Note that (1) is not symmetric and does not allow mass splitting, i.e., for some $\mathbb{P}, \mathbb{Q} \in P(X), P(Y)$, there cannot be any T satisfying $T_\# P = Q$. Thus, (Kantorovitch, 1958) proposed the following relaxation:

$$Cost(\mathbb{P}, \mathbb{Q}) = \inf_{\pi \in \Pi(\mathbb{P}, \mathbb{Q})} \int_{\chi \times y} c(x, y)\, d\pi(x, y) \tag{2}$$

where the minimum is taken over all transportation plans π(Figure 2a), i.e., distributions on $X \times Y$ whose marginals are $\mathbb{P}$ and $\mathbb{Q}$. The optimal $\pi\star \in \Pi(\mathbb{P}, \mathbb{Q})$ is called the optimal transportation plan. If $\pi\star$ is of the form $[id, T\star]$ $\mathbb{P} \in \Pi(\mathbb{P}, \mathbb{Q})$ for some $T\star$, then $T\star$ minimizes (1). In this case, the plan is called deterministic. Otherwise, it is called stochastic.

An example of OT cost for $X = Y = \mathbb{R}^D$ is the (p power of) Wasserstein p distance W_p, i.e., the formulation (2) with $c(x, y) = \|x - y\|^p$. Two of its most popular cases are $p = 1, 2(\mathbb{W}_1, \mathbb{W}_2^2)$.

Weak OT Formulation (Gozlan et al., 2017). Let $C : X \times P(Y) -> \mathbb{R}$ be a weak cost, i.e., a function which takes as

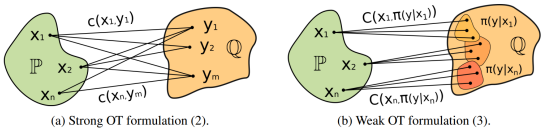

(a) Strong OT formulation (2). (b) Weak OT formulation (3).

Figure 2. Strong (Kantorovitch, 1958) and weak (Gozlan et al., 2017) optimal transport fomulations

input a point $x \in \chi$ and a distribution of $y \in Y$. The weak OT cost between $\mathbb{P}, \mathbb{Q}$ is

$$Cost(\mathbb{P}, \mathbb{Q}) = \inf_{\pi \in \Pi(\mathbb{P}, \mathbb{Q})} \int_\chi C(x, \pi(\cdot|x))\, d\pi(x) \tag{3}$$

where $\pi(\cdot|x)$ denotes the conditional distribution (Figure 3b). Note that (3) is a generalization of (2). In fact, for the cost $C(x, \mu) = \int_Y c(x, y)\, d\mu(y)$, the weak formulation (3) becomes the strong formulation (2). An example of a weak OT cost for $X = Y = \mathbb{R}^D$ is the γ-weak ($\gamma \geq 0$) Wasserstein-2 (W_2, γ):

$$C(x, \mu) = \int_Y \frac{1}{2}\|x - y\|^2 d\mu(y) - \frac{\gamma}{2} Var(\mu) \tag{4}$$

Existence and duality. Throughout the paper, we consider weak costs C(x, μ) which are bounded, convex in μ, and jointly lower semicontinuous. bounded, convex in μ, and jointly lower semicontinuous in an appropriate sense. Under these assumptions, (Backhoff-Veraguas et al., 2019) proves that the minimizer π^* of of (3) always exists. With mild assumptions on c, strong costs satisfy these assumptions. In particular, they are linear with respect to μ, and thus convex. The γ-weak quadratic cost (4) is lower bounded (for $\gamma \leq 1$) and also convex, since the function Var(μ) is concave in μ. For the costs in question, the dual form of (3) is

$$Cost(\mathbb{P}, \mathbb{Q}) = \sup_f \int_X f^C(x) d\mathbb{P}(x) + \int_Y f(y) d\mathbb{P}(y) \tag{5}$$

where f are the upper bounded continuous functions with not very fast growth (Backhoff-Veraguas et al., 2019) and f^C is the weak C-transform of f, i.e.

$$f^C(x) \stackrel{def}{=} \inf_{\mu \in P(Y)} \{C(x, \mu) - \int_Y f(y) d\mu(y)\} \tag{6}$$

Note that for strong costs C, the infimum is reached at every $\mu \in P(Y)$ supported on the $arg\inf_{y \in Y}\{c(x, y) - f(y)\}$ set. Therefore, it is sufficient to use the strong c-transform:

$$f^C(x) = f_c(x) \stackrel{def}{=} \inf_{y \in Y} \{c(x, y) - f(y)\}. \tag{7}$$

For strong costs (2), formula (5) with (7) is the well-known Kantorovich duality (Villani, 2008). In this project, we use two neural networks: ResNet and Unet.A residual neural network (ResNet) is an artificial neural network (ANN). It is a gateless or open-gated variant of the HighwayNet, the first working very deep feedforward neural network with hundreds of layers, much deeper than previous neural networks. The Unet network is based on the fully convolutional network, and its architecture has been modified and extended to work with fewer training images and to produce more accurate segmentations.

2.1. Dataset and preprocessing

In this section, we explain the datasets that we use. The first dataset is shoes, provided by Yu and Grauman. It is a large shoe dataset consisting of 50K catalog images collected from Zappos.com (reference to dataset). The images are divided into 4 major categories - shoes, sandals, slippers, and boots - followed by functional types and individual brands. Shoes are centered on a white background and shown in the same orientation for ease of analysis. Another dataset of 137K handbag images is downloaded from Amazon (reference to dataset). In both datasets, the images have 3 RGB channels with size 64x64 pixels. After loading the datasets, we apply normalization to them. Then we divide the data into training part (90 % of the whole dataset) and test part (10 % of the whole dataset).

2.2. Training parameters and metric

To train the Unet and ResNet models, we use a learning rate of 10^{-4}, a weight decay of 10^{-10}, and a batch size of 128. The training of the models was done as follows, each iteration of the model consisted of 10000 epochs. In our project we implemented 3 iterations. To evaluate the accuracy of the obtained result, the metric FID is used. FID is a measure of similarity between two sets of images. It has been shown to correlate well with human judgment of visual quality and is most commonly used to evaluate the quality of Generative Adversarial Network samples. FID is calculated by computing the Fréchet distance between two Gaussians fitted to feature representations of the Inception network.

The formula for calculating the Fréchet inception distance, which is used to access the quality of generated images, is

$$FID = \|\mu - \mu_w\| + tr(\sum + \sum_w -2(\sum \sum_w)^{\frac{1}{2}} \quad (8)$$

where $N(\mu, \sum)$ is the multivariate normal distribution estimated from Inception v3 (Szegedy et al., 2016) features computed on real images and $N(\mu_w, \sum_w)$ is the multivariate normal distribution estimated from Inception v3 features computed on generated (fake) images. The metric was originally proposed in (Szegedy et al., 2016).

Using the default feature extraction (Inception v3 with the original weights from (Heusel et al., 2017)), the input is expected to be mini-batches of 3-channel RGB images of the form $(3 \times H \times W)$.

The stacking procedure is summarized in the following diagram 3. A stacking iteration consists of training T and f and then applying T to create a new data set.

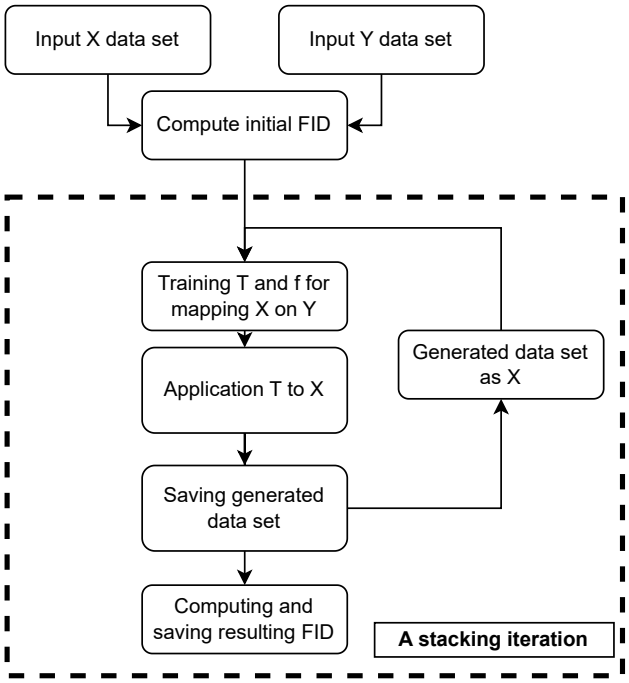

Figure 3. Scheme of stacking. Input X data set is shoes and input Y data set is bags.

3. Related work

In large-scale machine learning, OT costs are primarily used as a loss to learn generative models. Wasserstein GANs introduced by (Arjovsky et al., 2017; Gulrajani et al., 2017) are the most popular examples of this approach. We refer to (Korotin et al., 2022; 2021a) for recent surveys of the principles of GANs. However, these models are beyond the scope of our paper, since they only compute OT costs, but not OT plans or maps (4.3). Computing OT plans (or maps) is a more challenging problem, and only a limited number of scalable methods have been developed to solve it. In the following, we review methods for computing OT plans (or maps). We emphasize that existing methods are only designed for strong OT formulations (2). Most of them search for a deterministic solution (1), i.e. a map $T^\star$, rather than a stochastic plan $\pi^\star$, although $T^\star$ may not

always exist. To compute the OT plan (map), (Lu et al., 2020; Xie et al., 2019) approach the primal formulation (1) or (2). Their methods imply the use of generative models and yield complex optimization objectives with multiple adversarial regularizers, e.g., they are used to enforce the boundary condition ($T_{\#}P = Q$). As a result, these methods are difficult to tune because they require careful selection of hyperparameters. In contrast, methods based on the dual formulation (5) have simpler optimization procedures. Most of these methods are designed for OT with quadratic cost, i.e., Wasserstein-2 distance ($\mathbb{W}_2^2$). An evaluation of these methods is given in (Korotin et al., 2021a).Below we mention their problems. Methods (Taghvaei & Jalali, 2019; Makkuva et al., 2020; Korotin et al., 2021a) based on input-convex neural networks (ICNNs, see (Amos et al., 2017)) have a solid theoretical justification, but do not provide sufficient performance in practical large-scale problems. Methods based on entropy regularized OT (Genevay et al., 2016; Seguy et al., 2017), recover regularized OT map that is biased from the true one, it is difficult to sample from it or compute its density. According to (Korotin et al., 2021b), the best performing approach is $[MM : R]$, which is based on the maximin reformulation of (5). It recovers OT maps quite well and has a good generative performance. The follow-up papers (Rout et al., 2021; Fan et al., 2021) test extensions of this approach for more general strong transport costs c$(\cdot, \cdot)$ and apply it to the computation of $\mathbb{W}_2$ barycenters (Korotin et al., 2022). Its main limitation is that it aims to recover a deterministic OT map T^*, which may not exist.

Therefore, we solve the reformulation task instead of the min task. It recovers OT maps quite well and has a good generative performance. The min-max formulation looks like this:

$$Cost(\mathbb{P}, \mathbb{Q}) = \sup_{f} \inf_{T} \mathcal{L}(f, T) \tag{9}$$

where $L(f, T)$ is next:

$$\mathcal{L}(f, T) = \int \frac{\|x - T(x)\|_2^2}{2} d\mathbb{P}(x) + \int f(y)\, d\mathbb{Y} - \int f(T(x))\, d\mathbb{P}(x) \tag{10}$$

After reformulating our problem, we applied UNet for T function and ResNet for f with initiated weights. During a training cycle, we fix f terms in the loss function and at the same time look for the minimum of the T term, which is UNet for kind of generation. Furthermore, a new data set was received from Unet, which was used for further ResNet training. Having found the minimum of the first term, we fix it and start looking for the maximum of the function responsible for Reset for the kind of discrimination. Then we repeat all the steps until we find the saddle point.

4. Experiments and Results

	Min FID	Mean FID	Std FID
Iteration 1	35.0	43.9	9.5
Iteration 2	26.1	34.7	4.8
Iteration 3	37.9	44.6	2.1

Table 1. FID Scores

We did several iterations of stacking. And as you can see after about 10k epochs of the first iteration there is a plateau and almost no improvement of the FID metrics. The minimum FID at the first iteration is 34.9. The images of the bags obtained after the first iteration are quite similar to the real ones, although there are significant artifacts.

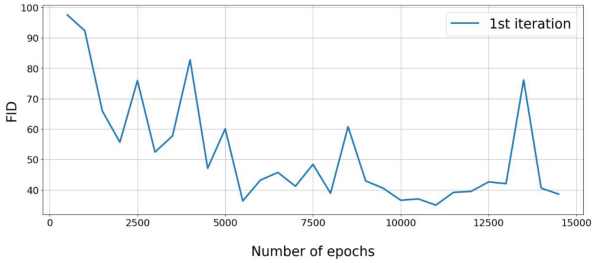

Figure 4. FID metric of the first iteration. Shoes to Bags minimal FID is 34.9.

Figure 5. Result of first iteration. Shoes to Bags min FID is 34.9

We then proceeded to the second iteration and succeeded in achieving a smaller FID - 26.2. The FID metric in the first stacking behaves more smoothly without such peaks, but continues to oscillate. Here we obtained a significant improvement in style transfer, as the resulting images of the bags had fewer artifacts and began to look more realistic.

The last third iteration has almost no change in the FID metrics, and moreover it shows a worse result than the previous iterations. If we look at the resulting images 9, we see that the images obtained in the previous iteration are almost indistinguishable from the images of the last iteration.

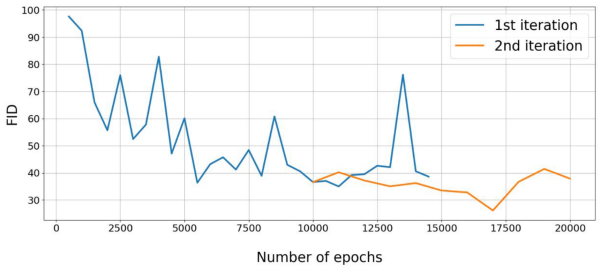

Figure 6. Result of second iteration. Bags from shoes to Bags min FID is 26.2 (orange line)

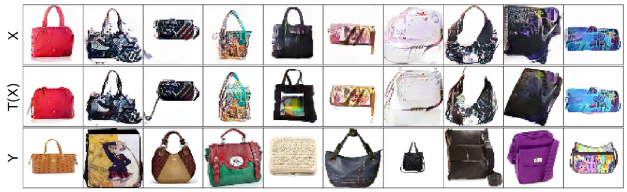

Figure 7. Bags from shoes to Bags min FID is 26.2

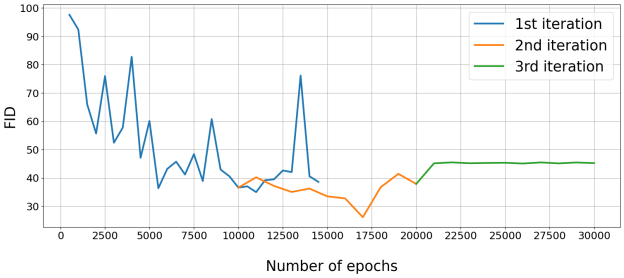

Figure 8. The main results of the work. The graph shows the dependence of the number of epochs on the FID metric.Bags from the first stack to bags min FID is 38.9

5. Conclusion

With zero levels of stacking the FID is equal to 34.9. With one level of stacking the min FID is 26.2, which is reduced compared to the previous results, giving us a good mapping as output. And finally, two levels of stacking result in FID 38.9, which is much higher than the one level of stacking. Final conclusions about this experiment can’t be made, since it requires explorations with a greater number of levels.

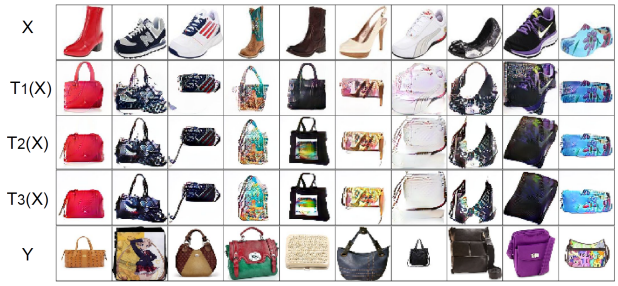

Figure 9. The main results of the work.Bags from the first stack to bags min FID is 38.9

References

Amos, B., Xu, L., and Kolter, J. Z. Input convex neural networks. In *International Conference on Machine Learning*, pp. 146–155. PMLR, 2017.

Arjovsky, M., Chintala, S., and Bottou, L. Wasserstein generative adversarial networks. In *International conference on machine learning*, pp. 214–223. PMLR, 2017.

Backhoff-Veraguas, J., Beiglböck, M., and Pammer, G. Existence, duality, and cyclical monotonicity for weak transport costs. *Calculus of Variations and Partial Differential Equations*, 58(6):203, 2019.

Fan, J., Liu, S., Ma, S., Chen, Y., and Zhou, H. Scalable computation of monge maps with general costs. *arXiv preprint arXiv:2106.03812*, pp. 4, 2021.

Genevay, A., Cuturi, M., Peyré, G., and Bach, F. Stochastic optimization for large-scale optimal transport. *Advances in neural information processing systems*, 29, 2016.

Gozlan, N., Roberto, C., Samson, P.-M., and Tetali, P. Kantorovich duality for general transport costs and applications. *Journal of Functional Analysis*, 273(11):3327–3405, 2017.

Gulrajani, I., Ahmed, F., Arjovsky, M., Dumoulin, V., and Courville, A. C. Improved training of wasserstein gans. *Advances in neural information processing systems*, 30, 2017.

Heusel, M., Ramsauer, H., Unterthiner, T., Nessler, B., and Hochreiter, S. Gans trained by a two time-scale update rule converge to a local nash equilibrium. *Advances in neural information processing systems*, 30, 2017.

Kantorovitch, L. On the translocation of masses. *Management science*, 5(1):1–4, 1958.

Korotin, A., Li, L., Genevay, A., Solomon, J. M., Filippov, A., and Burnaev, E. Do neural optimal transport solvers work? a continuous wasserstein-2 benchmark. *Advances in Neural Information Processing Systems*, 34:14593–14605, 2021a.

Korotin, A., Li, L., Solomon, J., and Burnaev, E. Continuous wasserstein-2 barycenter estimation without minimax optimization. *arXiv preprint arXiv:2102.01752*, 2021b.

Korotin, A., Selikhanovych, D., and Burnaev, E. Neural optimal transport. *arXiv preprint arXiv:2201.12220*, 2022.

Liu, M.-Y., Breuel, T., and Kautz, J. Unsupervised image-to-image translation networks. *Advances in neural information processing systems*, 30, 2017.

Lu, G., Zhou, Z., Shen, J., Chen, C., Zhang, W., and Yu, Y. Large-scale optimal transport via adversarial training with cycle-consistency. *arXiv preprint arXiv:2003.06635*, 2020.

Makkuva, A., Taghvaei, A., Oh, S., and Lee, J. Optimal transport mapping via input convex neural networks. In *International Conference on Machine Learning*, pp. 6672–6681. PMLR, 2020.

Petzka, H., Fischer, A., and Lukovnicov, D. On the regularization of wasserstein gans. *arXiv preprint arXiv:1709.08894*, 2017.

Rout, L., Korotin, A., and Burnaev, E. Generative modeling with optimal transport maps. *arXiv preprint arXiv:2110.02999*, 2021.

Sanjabi, M., Ba, J., Razaviyayn, M., and Lee, J. D. On the convergence and robustness of training gans with regularized optimal transport. *Advances in Neural Information Processing Systems*, 31, 2018.

Seguy, V., Damodaran, B. B., Flamary, R., Courty, N., Rolet, A., and Blondel, M. Large-scale optimal transport and mapping estimation. *arXiv preprint arXiv:1711.02283*, 2017.

Szegedy, C., Vanhoucke, V., Ioffe, S., Shlens, J., and Wojna, Z. Rethinking the inception architecture for computer vision. In *Proceedings of the IEEE conference on computer vision and pattern recognition*, pp. 2818–2826, 2016.

Taghvaei, A. and Jalali, A. 2-wasserstein approximation via restricted convex potentials with application to improved training for gans. *arXiv preprint arXiv:1902.07197*, 2019.

Villani, C. Optimal transport, old and new. notes for the 2005 saint-flour summer school. *Grundlehren der mathematischen Wissenschaften [Fundamental Principles of Mathematical Sciences]. Springer*, 3, 2008.

Xie, Y., Chen, M., Jiang, H., Zhao, T., and Zha, H. On scalable and efficient computation of large scale optimal transport. In *International Conference on Machine Learning*, pp. 6882–6892. PMLR, 2019.

A. Team member's contributions

Explicitly stated contributions of each team member to the final project.

Daniil Panov (22% of work)

- Coding a part of stacking section
- Experiments on the first iteration of the stacking
- Preparing the GitHub Repo
- General reviewing and editing of the report
- Preparation of the project presentation

Nikita Bogdanov (22% of work)

- Coding a part of stacking section
- Experiments on the all iteration of the stacking
- Contributing to the GitHub Repo
- Editing of the experiments and Results and reviewing other sections
- Preparation of the project presentation

Nikolay Kashin (18% of work)

- Participating in group discussions
- Editing of the experiments and Results and reviewing other sections
- Preparation of the project presentation

Anastasia Gavrish (19% of work)

- Writing report
- Contributing to the GitHub Repo
- Participating in group discussions

Nikita Vasilev (19% of work)

- Writing report
- Contributing to the GitHub Repo
- Participating in group discussions

B. Reproducibility checklist

Answer the questions of following reproducibility checklist. If necessary, you may leave a comment.

1. A ready code was used in this project, e.g. for replication project the code from the corresponding paper was used.

   - [x] Yes.
   - [ ] No.
   - [ ] Not applicable.

   General comment: If the answer is **yes**, students must explicitly clarify the stacking piplene was implemented. We deeply investigate the ready code and add around 20%.

   Students' comment: None

2. A clear description of the mathematical setting, algorithm, and/or model is included in the report.

   - [x] Yes.
   - [ ] No.
   - [ ] Not applicable.

   Students' comment: None

3. A link to a downloadable source code, with specification of all dependencies, including external libraries is included in the report.

   - [x] Yes.
   - [ ] No.
   - [ ] Not applicable.

   Students' comment: None

4. A complete description of the data collection process, including sample size, is included in the report.

   - [x] Yes.
   - [ ] No.
   - [ ] Not applicable.

   Students' comment: None

5. A link to a downloadable version of the dataset or simulation environment is included in the report.

   - [x] Yes.
   - [ ] No.
   - [ ] Not applicable.

   Students' comment: None

6. An explanation of any data that were excluded, description of any pre-processing step are included in the report.

   - [x] Yes.
   - [ ] No.
   - [ ] Not applicable.

   Students' comment: None

7. An explanation of how samples were allocated for training, validation and testing is included in the report.

   - [x] Yes.
   - [ ] No.
   - [ ] Not applicable.

   Students' comment: None

8. The range of hyper-parameters considered, method to select the best hyper-parameter configuration, and specification of all hyper-parameters used to generate results are included in the report.

   - [ ] Yes.
   - [ ] No.
   - [x] Not applicable.

   Students' comment: We were suggested not to modify hyper-parameters of the NN. Thus, creating and evaluation of the stacking pipline was done.

9. The exact number of evaluation runs is included.

   - [x] Yes.
   - [ ] No.
   - [ ] Not applicable.

   Students' comment: None

10. A description of how experiments have been conducted is included.

    - [x] Yes.
    - [ ] No.
    - [ ] Not applicable.

    Students' comment: None

11. A clear definition of the specific measure or statistics used to report results is included in the report.

    - [x] Yes.
    - [ ] No.
    - [ ] Not applicable.

    Students' comment: None

12. Clearly defined error bars are included in the report.

    - [x] Yes.
    - [ ] No.
    - [ ] Not applicable.

    Students' comment: None

13. A description of the computing infrastructure used is included in the report.

    - [x] Yes.
    - [ ] No.
    - [ ] Not applicable.

    Students' comment: None